

Geochemistry, Geophysics, Geosystems

RESEARCH ARTICLE

10.1029/2021GC009730

Special Section:

Clumped Isotope Geochemistry: From Theory to Applications

Key Points:

- Considerable oxygen isotope exchange occurs between internal water and biogenic carbonates during heating, which is less prevalent in inorganic carbonates
- The oxygen isotope exchange during heating leads to elevated clumped-isotope temperatures in biogenic aragonite
- Isotope resetting occurs at temperatures below the threshold for solid-state reordering without any detectable changes in mineralogy

Supporting Information:

Supporting Information may be found in the online version of this article.

Correspondence to:

H. J. L. van der Lubbe,
h.j.l.vander.lubbe@vu.nl

Citation:

Nooitgedacht, C. W., van der Lubbe, H. J. L., Ziegler, M., & Staudigel, P. T. (2021). Internal water facilitates thermal resetting of clumped isotopes in biogenic aragonite. *Geochemistry, Geophysics, Geosystems*, 22, e2021GC009730. <https://doi.org/10.1029/2021GC009730>

Received 22 FEB 2021

Accepted 30 APR 2021

© 2021. The Authors.

This is an open access article under the terms of the [Creative Commons Attribution](#) License, which permits use, distribution and reproduction in any medium, provided the original work is properly cited.

Internal Water Facilitates Thermal Resetting of Clumped Isotopes in Biogenic Aragonite

C. W. Nooitgedacht¹ , H. J. L. van der Lubbe¹ , M. Ziegler² , and P. T. Staudigel³ 

¹Department of Earth Sciences, Geology and Geochemistry, Vrije Universiteit Amsterdam, Amsterdam, The Netherlands, ²Department of Earth Sciences, Utrecht University, Utrecht, The Netherlands, ³School of Earth and Environmental Sciences, Cardiff University, Cardiff, UK

Abstract Biogenic and inorganic calcium carbonates contain considerable amounts of internal water, both as free and organically associated water. The oxygen isotopic compositions ($\delta^{18}\text{O}$) of internal water and hosting carbonate are analyzed for various carbonates before and after heating at 175°C for 90 minutes. During heating, the $\delta^{18}\text{O}$ values of internal water significantly increased in biogenic aragonites and speleothem calcite, whereas the $\delta^{18}\text{O}$ carbonate values were lowered. Correspondingly, an aragonitic bivalve's clumped-isotope distribution (Δ_{47}) changed during heating, increasing reconstructed paleotemperatures. In contrast, an inorganic aragonite crystal, containing a comparable amount of internal water, showed no oxygen isotope exchange, and its Δ_{47} values remained unaltered during heating, implying that there is a link between internal oxygen isotope exchange and Δ_{47} resetting. This alteration process occurred without any detectable transformation from aragonite to calcite. Our results therefore reveal a mechanism that facilitates oxygen isotope exchange between biogenic aragonite and its internal water, while simultaneously resetting the Δ_{47} values, without affecting mineralogy. Future studies may therefore apply coupled water-carbonate analyses to scrutinize these kinds of diagenetic alteration processes. It appears that in biogenic aragonites, more carbonate is available for exchange reactions with the internal water reservoir than in inorganic aragonites, a feature that can be attributed to the distribution of organic-associated water and/or high surface area fluid inclusions. This water-aragonite exchange occurs at lower temperatures than those required for solid-state bond reordering at the same timescale, and thus likely has occurred earlier during the burial of biogenic aragonites.

Plain Language Summary Calcium carbonate minerals are formed by both inorganic (e.g., speleothems) and biological processes (e.g., bivalve shells). During precipitation, small amounts of water are trapped in microscopic pores and/or associated organic components. Isotopic analyses of both carbonate and fluid inclusions before and after heating at 175°C for 90 minutes demonstrate that oxygen isotopes reequilibrated between both phases without the mineralogical transformation to calcite, a common first indicator of sample alteration. This outcome is unexpected and has implications for researchers, who wish to reconstruct the temperatures and isotopic compositions of waters from which these carbonates precipitated in the near and geological past.

1. Introduction

Primary marine and terrestrial carbonates consist predominantly of two polymorphs of calcium carbonate: calcite and aragonite. The relative abundance of these minerals has varied over 100 myr timescales (Sandberg, 1983; Zhang et al., 2020) due to changes in water chemistry and surface temperature (Adabi, 2004; Balthasar & Cusack, 2014). Despite being a common mineral at the Earth's surface, aragonite is metastable at surface temperatures and pressures and only becomes the more stable crystalline arrangement with significant substitution of ions (Carlson, 1980) and/or at elevated pressure at burial depths (Hacker, 2005). Because of this metastability, aragonite is more susceptible to chemical alteration, and thus its preservation is considered an indicator of pristine geochemistry (Stahl & Jordan, 1969). There is considerable variability in the response of different aragonite materials to alteration processes, which are related to differences in chemical composition and porosity (Pederson et al., 2020). The alteration typically involves the dissolution of aragonite and reprecipitation of the more stable polymorph calcite (Bischoff & Fyfe, 1968), a process termed neomorphism (Folk, 1965).

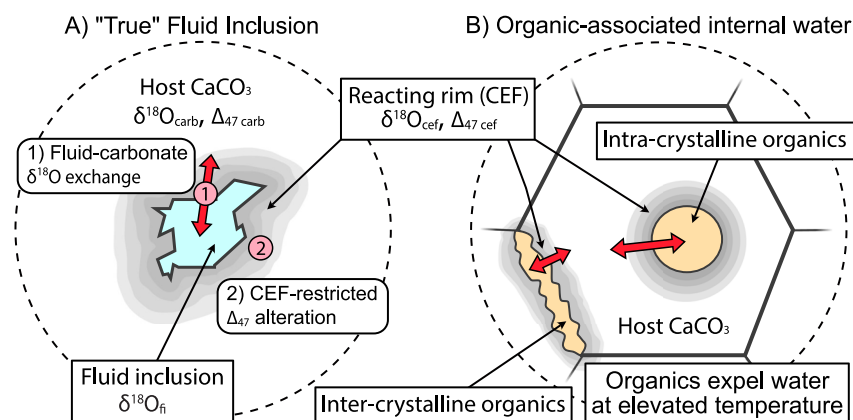


Figure 1. Schematic representation of (a) a fluid inclusion in carbonate (i.e., liquid water trapped in carbonate) and (b) organic-associated internal water in carbonate (i.e., carbonate bound to inter- and intracrystalline organic material). Hypothetically, the gray rim that surrounds the fluid inclusion, the Carbonate Exchange Fraction (CEF), marks the location where (1) oxygen isotope ($\delta^{18}\text{O}$) exchange by microscopic dissolution-precipitation reactions occurs and (2) the clumped-isotope (Δ_{47}) thermometer is reset (modified from Uemura et al., 2019 and Nooitgedacht et al., 2021).

The exchange of isotopes between carbonate and ambient fluids during the aragonite to calcite transition commonly results in an isotopic shift toward the equilibrium $\delta^{18}\text{O}$ values of the newly formed calcite. In the presence of an experimental “diagenetic fluid,” it was shown that calcite formation is accelerated and initiates at 160°C–200°C on experimental timescales (Casella et al., 2017; Milano et al., 2016; Pederson, Mavromatis, et al., 2019; Pederson, Weiss, et al., 2019; Pederson et al., 2020). This reaction rate is considerably accelerated and occurs at lower temperatures if a powdered aragonite is used in the alteration experiment (Guo et al., 2019). Dry heating (or “roasting”) experiments revealed that the transition to calcite requires more time and/or higher temperatures, but is nevertheless accompanied by an oxygen isotopic shift in the carbonate (Milano et al., 2018; Müller, Staudigel, et al., 2017; Staudigel & Swart, 2016). This isotopic shift, which occurs in absence of interaction with an outside medium, is believed to be caused by a set of exchange reactions that occur with internal fluids (Moon et al., 2020; Pederson, Mavromatis, et al., 2019; Pederson, Weiss, et al., 2019; Uemura et al., 2019), and/or internal organic material (Li et al., 2020).

While it is generally understood that exchange reactions occur when new minerals are formed, it was suggested that the isotopic depletion that typically accompanies the aragonite transition may occur also in the absence of detectable mineralogical conversion in roasted aragonite samples (Müller, Staudigel, et al., 2017; Staudigel & Swart, 2016). Recent experiments show that while a bulk oxygen isotope shift occurs within aragonite shell carbonate at relatively low (200°C) temperatures, internal heterogeneity is preserved in the form of seasonal banding (Moon et al., 2020). These internal exchange reactions could be between carbonates and internal fluids (Figure 1a), and/or the waters bound to inter- and/or intracrystalline organic materials (Figure 1b). Thermogravimetric and IR absorption experiments reveal that there are considerable volumes (~2 wt%–3 wt%) of water released as biogenic aragonites are heated associated with both free water and organically associated water (Cuif et al., 2004). These results call into question the commonly used standards for assessing pristine aragonite material and stress the potential influence of microscale diagenesis in fossil aragonite archives.

Clumped-isotope analyses of biogenic aragonite materials that were heated (Müller, Staudigel, et al., 2017; Staudigel & Swart, 2016) have revealed that biogenic aragonite is more susceptible to internal resetting of clumped isotopes (Δ_{47}) than calcite (Passey & Henkes, 2012) or abiogenic aragonite (Chen et al., 2019). This susceptibility to alteration at lower temperatures has provided a potentially useful tool for reconstructing the thermal histories of aragonitic bivalves found in archeological contexts, giving insight into ancient cooking methods (Müller, Staudigel, et al., 2017; Staudigel et al., 2019). For inorganic aragonite, it was found that clumped-isotope resetting is intrinsically associated with the solid-state transition from aragonite to calcite (Chen et al., 2019), whereas the biogenic aragonites’ Δ_{47} values invariably altered at a lower temperature than the threshold for the mineral transition (Müller, Staudigel, et al., 2017; Staudigel & Swart, 2016). More recently, it was proposed that clumped-isotope resetting in gastropod fossils occurred at very low

temperatures during winter freezing (Wang et al., 2020); an observation which, if true, would represent a previously unexplored form of alteration for clumped isotopes in visually unaltered aragonite fossil samples. The interpretation of these observations requires a better mechanistic understanding of why biogenic aragonite materials behave so differently from abiogenic aragonite or other common carbonate minerals. Due to the cooccurring change in carbonate $\delta^{18}\text{O}$ values, it has been speculated that Δ_{47} -resetting in biogenic aragonites may be related to isotopic exchange with the host carbonate's internal fluids (Staudigel et al., 2019; Staudigel & Swart, 2016), however, this theory has remained unverified experimentally. Here, we present a series of experiments, wherein the oxygen isotopes of fluid inclusion were measured in a range of natural aragonitic and calcite materials before and after a heating experiment (175°C for 90 minutes). In conjunction, clumped and stable isotope measurements were performed on a subset of these samples, examining the link between internal isotope exchange and the resetting of clumped isotopes in aragonite.

A recent study investigated the covariance of fluid inclusion and host calcite oxygen isotope ratios as well as clumped isotopes of carbonate veins (Nooitgedacht et al., 2021). The oxygen isotope fractionation factor (α_{c-fi}) between host carbonate ($\delta^{18}\text{O}_c$) and internal fluid ($\delta^{18}\text{O}_f$) allows CaCO_3 precipitation temperature estimates assuming that precipitation took place in isotopic equilibrium (e.g., Coplen, 2007; Daëron et al., 2019; Kim & O'Neil, 1997; Staudigel & Swart, 2018; Tremaine et al., 2011; Yan et al., 2012). The derived paleotemperatures from the carbonate-fluid $\delta^{18}\text{O}$ paleothermometer ($T\alpha_{c-fi}$) were highly discrepant with those obtained by the Δ_{47} -paleothermometer ($T\Delta_{47}$), suggesting that fluid inclusions had exchanged isotopes with the vein carbonate during millions of years of exhumation. The offset between paleothermometers suggested isotope exchange between fluid inclusions and host calcite had been restricted to a fraction of the total vein carbonate. The same idea was previously put forward by a heating experiment of speleothem calcite (Uemura et al., 2019). The fraction of calcite that is available for oxygen isotope exchange with the fluid inclusions has been termed as the Calcite Exchange Fraction (CEF; Nooitgedacht et al., 2021, Figure 1). This CEF, which is expected to vary between materials, could potentially explain the difference between inorganic and organic carbonate's response to thermal alteration experiments: if in inorganic aragonite, less CaCO_3 is available for isotopic exchange (i.e., low CEF) than in biogenic aragonite, possibly reflecting a relatively low mineral-fluid contact area or permeability, then fluid-carbonate exchange is minimized and results in little change in Δ_{47} and $\delta^{18}\text{O}$ fluid values. Conversely, if biogenic aragonite has a higher CEF, possibly indicating higher surface area or more connected pores, then one would expect greater changes in Δ_{47} and $\delta^{18}\text{O}$ values during heating experiments. In the case of organic-rich carbonates such as coral skeletons and bivalve shells, the bulk crystalline material is interwoven with organic matter including hydrated proteoglycans, which decompose during heating above 60°C–100°C (Dauphin et al., 2006); if these hydrated proteins are a source of oxygen for exchange with the carbonate minerals, these would be very well-distributed despite comprising only a small fraction of the total mass. At present, these physical explanations for differences in the CEF are mostly speculative, and a better understanding of this will require additional analyses of different materials using clumped isotopes and mineralogical determinations.

2. Methods

2.1. Sample Selection and Experimental Design

In order to investigate the link between clumped-isotope resetting and carbonate-fluid interaction and the potential role that the type of calcium carbonate material plays in the magnitude of this effect, a variety of calcium carbonate samples were subjected to a heating experiment. The samples consist of (1) an aragonite warm-water coral (*Hexagonaria*; collection Vrije Universiteit (VU) Amsterdam), (2) inorganic single-crystal "Moroccan Aragonite" (mineral trade), (3) Holocene speleothem calcite from the Scladina cave in Belgium (de Graaf et al., 2020), (4) an aragonitic giant clam (Tridacninae; presumably *Hippopus Porcellanus*; antique trade), and (5) an aragonitic land snail endemic to the Philippines (*Ryssota otaheitana*; decoration trade). From each sample, eight subsamples were cut, cleaned, weighed, and divided into two groups of equal size. The biogenic samples were drilled along the periodic growth lines to minimize sample heterogeneity. Drills and sawblades were cooled and operated carefully to avoid unnecessary heating, to avoid affecting sample mineralogy and Δ_{47} values (Staudigel & Swart, 2016). One group of each sample was measured directly for fluid inclusion stable isotope ratios of hydrogen and oxygen, the other was heated to 175°C in an oven for

90 minutes prior to the fluid inclusion analysis. Hereafter, subsamples were powdered gently with a mortar and pestle by hand to reduce thermal friction before the carbonate stable isotopes and Δ_{47} measurements.

2.2. Fluid Inclusion Stable Isotope Analysis

The fluid inclusion isotope ratios of oxygen ($\delta^{18}\text{O}_{\text{fi}}$), as well as hydrogen ($\delta^2\text{H}_{\text{fi}}$), were measured using an updated version of the Amsterdam Device (Vonhof et al., 2006) at the Earth Sciences Stable Isotope Laboratory at the VU Universiteit Amsterdam. The Amsterdam Device consists of two identical online crusher chambers that are connected in parallel to a Temperature Conversion Elemental Analyzer (TC-EA) pyrolysis furnace. In the crusher chambers, a carbonate sample is crushed by a hardened steel piston at 110°C and the sample's internal fluids are released to a cold-trap unit, where H_2O is isolated and focused. A flash heater releases the trapped water sample into the high TC-EA, which converts the water sample into hydrogen and carbon monoxide gas, which are measured by a ThermoFinnigan Delta + Isotope Ratio Mass Spectrometer (IRMS) for their hydrogen and oxygen isotopic compositions. For this setup, the reproducibility of routinely analyzed water standards (ALW11 and KONA; Data Set S1) is 0.8‰ for hydrogen and 0.1‰ for oxygen, relative to the V-SMOW scale. The fluid inclusion results were validated by comparison of the Sciadina speleothem unheated samples against IRMS and Cavity Ring-down Spectrometer (CRDS) results of the same record ($\delta^2\text{H}_{\text{fi}}$: -42.4 ± 1.67 , $\delta^{18}\text{O}_{\text{fi}}$: -6.5 ± 0.64 ‰) as reported by de Graaf et al., (2020).

2.3. X-Ray Diffraction, Clumped, and Stable Isotope Analysis of Carbonate

The $\delta^{13}\text{C}$ and $\delta^{18}\text{O}$ values of all subsamples were analyzed by Thermo Scientific MAT253-plus equipped with a Gasbench II at the Earth Sciences Stable Isotope Laboratory at the VU. Samples were digested in phosphoric acid at 45°C. Routine measurements of carbonate standard IAEA-603 were performed with a precision below 0.1‰ for both $\delta^{13}\text{C}$ and $\delta^{18}\text{O}$. The Δ_{47} composition and mineralogy (XRD) of heated (H) and unheated (UH) equivalents of single-crystal “Moroccan” inorganic aragonite and bivalve biogenic aragonite (Moroc_H1; Moroc_UH3; SHELL5_H2; SHELL4_UH1) were analyzed at the Stable Isotope Laboratory of the Utrecht University (UU); Appendixes A and B). The $\delta^{13}\text{C}$ and $\delta^{18}\text{O}$ values of these samples were therefore measured at both laboratories. Subsamples of ~ 80 μg were prepared and analyzed by a Thermo Scientific MAT253-Plus connected to a KIEL IV sample preparation device. During the analytical procedure, calcite was dissolved in phosphoric acid at 70°C (Meckler et al., 2014) to produce CO_2 . Sample gas was filtered from contaminants by a cooled, -40°C Porapak column. Analyses were performed using the LIDI protocol (long-integration dual inlet mode), reducing sample size and analysis time (Müller, Fernandez, et al., 2017). Pressure baseline corrections (PBL) of the raw beam signal were performed based on daily peak shape scans in order to remove compositional artifacts (Meckler et al., 2014). The Δ_{47} values were calculated using the parameters of Brand et al., (2010) and Daëron et al., (2016) and were standardized using ETH-1, ETH-2, and ETH-3 international standards (Bernasconi et al., 2018). The ETH-3 standard was measured more often to reduce uncertainty limits (Kocken et al., 2019). Temperatures were calculated using the Bernasconi et al. (2018) Δ_{47} -temperature calibration. The long-term standard deviation over the course of the measurement period was 0.03‰.

2.4. Isotope Exchange Calculations

Calculations regarding the oxygen isotope exchange between calcite and internal fluids are based on the mass-balance equation for isotope batch fractionation (Gat & Gonfiantini, 1981), which was rewritten to:

$$\delta^{18}\text{O}_{\text{c}}^{\text{UH}} M_{\text{c}} + \delta^{18}\text{O}_{\text{fi}}^{\text{UH}} M_{\text{fi}} = \delta^{18}\text{O}_{\text{c}}^{\text{H}} M_{\text{c}} + \delta^{18}\text{O}_{\text{fi}}^{\text{H}} M_{\text{fi}} \quad (1)$$

In Equation 1, M_{c} refers to the molar quantity of oxygen in the carbonate phase and M_{f} to the molar quantity of oxygen in the fluid phase. The superscripts “UH” and “H” refer to the heated and unheated samples, respectively. Equation 1 was refined by Nooitgedacht et al., (2021) so that exchange between oxygen isotopes occurs only within the confines of CEF and exchange between fluid inclusions is temperature dependent, governed by the temperature-dependent fractionation factor α (e.g., Coplen, 2007; Daëron et al., 2019; Kim & O’Neil, 1997; Staudigel & Swart, 2018; Tremaine et al., 2011; Yan et al., 2012). The apparent fractionation of oxygen isotopes between carbonate and fluid inclusions is defined as follows:

Table 1
Isotopic Results of the Heating Experiment

Experimental results	Inorganic carbonate			Biogenic carbonate	
	Speleothem calcite	Moroccan aragonite	Aragonite shell (bivalve)	Aragonite coral	Aragonite snail
Unheated					
$\delta^2\text{H}$ fluid inclusion (‰SMOW)	-45.1 ± 4.2	-54.8 ± 2.5	-38.5 ± 7.3	-34.1 ± 4.1	-58.8 ± 2.6
$\delta^{18}\text{O}$ fluid inclusion (‰SMOW)	-7.3 ± 0.2	-8.8 ± 0.6	1.7 ± 2.3	0.8 ± 1.4	0.0 ± 1.1
$\delta^{13}\text{C}$ calcite (‰VPDB)	-9.51 ± 0.22	8.49 ± 0.05	2.53 ± 0.17	-1.76 ± 0.17	-14.16 ± 0.07
$\delta^{18}\text{O}$ calcite (‰VPDB)	-5.40 ± 0.09	-7.88 ± 0.05	-1.76 ± 0.04	-4.61 ± 0.07	-5.13 ± 0.08
$T\alpha_{c-fi}$ (°C; Kim & O'Neil, 1997)	6.6 ± 0.7	10.6 ± 1.9	32.2 ± 8.7	43.4 ± 5.6	40.7 ± 4.5
$T\Delta_{47}$ (°C)*		22.3 ± 15.5	31.9 ± 15.4		
Heated					
$\delta^2\text{H}$ fluid inclusion (‰SMOW)	-46.4 ± 3.9	-54.0 ± 9.6	-47.3 ± 4.2	-13.4 ± 4.7	-49.8 ± 6.0
$\delta^{18}\text{O}$ fluid inclusion (‰SMOW)	-6.7 ± 0.4	-7.6 ± 1.3	8.5 ± 0.7	6.7 ± 1.3	4.1 ± 0.7
$\delta^{13}\text{C}$ calcite (‰VPDB)	-9.92 ± 0.20	8.52 ± 0.07	2.48 ± 0.10	-1.78 ± 0.17	-14.12 ± 0.08
$\delta^{18}\text{O}$ calcite (‰VPDB)	-5.53 ± 0.07	-7.93 ± 0.05	-1.88 ± 0.5	-4.95 ± 0.07	-5.19 ± 0.05
$T\alpha_{c-fi}$ (°C; Kim & O'Neill, 1997)	8.6 ± 1.4	15.8 ± 4.5	70.7 ± 3.3	77.5 ± 6.4	64.5 ± 3.3
$T\Delta_{47}$ (°C)		19.7 ± 8.8	70.0 ± 19.2		
CEF (%)		-0.30 ± 1.40	39.40 ± 7.10		
<i>Two-tailed, paired t test for equal variance (p values)</i>					
$\delta^2\text{H}$ fluid inclusion	0.524	0.86	0.166	0.011*	0.101
$\delta^{18}\text{O}$ fluid inclusion	0.019*	0.266	0.017*	0.000*	0.014*
$\delta^{18}\text{O}$ calcite	0.033*	0.235	0.007*	0.001*	0.13
$\delta^{13}\text{C}$ calcite	0.01*	0.271	0.589	0.853	0.522
$T\Delta_{47}$ (°C)**		0.649	0.002*		

Note. *p* Values are reported for Student's *t* tests between the heated and unheated samples, whereby single asterisks denote significant changes in composition before and after heating. The double asterisks denote the *p* values in case a Welch's *t* test was performed. The plus-minus symbols represent 95% confidence intervals.

$$\alpha_{c-fi}^H = \frac{\delta^{18}\text{O}_c^H + 1,000\text{‰}}{\delta^{18}\text{O}_{fi}^H + 1,000\text{‰}} = \frac{\delta^{18}\text{O}_c^{\text{UH}}(1 - \text{CEF}) + \delta^{18}\text{O}_{\text{cef}}^H \text{CEF} + 1,000\text{‰}}{\delta^{18}\text{O}_{fi}^H + 1,000\text{‰}} \quad (2)$$

In Equation 2, the term that describes the composition of heated carbonate in Equation 1, ($\delta^{18}\text{O}_c^H$), is restricted by CEF and appears as $\delta^{18}\text{O}_{\text{cef}}^H$. The composition of calcite, $\delta^{18}\text{O}_c^H$, is described by averaging the isotope composition of the exchanged carbonate within CEF and the unaltered composition outside of CEF. The equilibrium fractionation of oxygen isotopes, $\alpha(T)$, varies according to a temperature-equilibrium equation such as those described above. In this study, we assess the apparent temperature offset ($\Delta T\alpha_{c-fi}$) between heated and unheated samples, using the Kim and O'Neil (1997) experimental temperature calibration (Table 1). Experimentally induced offsets in $T\alpha_{c-fi}$ between heated and unheated samples were recorded using a single temperature calibration.

The value of CEF can be calculated from Equation 2, but it requires accurate estimates of the molar fraction of oxygen present in fluid inclusions. Alternatively, CEF can be calculated based on the clumped-isotope measurements before and after heating:

$$\Delta_{47(m)} = \Delta_{47(\text{UH})}(1 - \text{CEF}) + \Delta_{47(\text{H})}(\text{CEF}) \quad (3)$$

in which $\Delta_{47(m)}$ represents the measured clumped-isotope temperature of the heated sample, which underwent the experimental treatment. $\Delta_{47(\text{UH})}$ represents the clumped-isotope composition of the unheated sample, and $\Delta_{47(\text{H})}$ defines the clumped-isotope composition of the altered material that sits within the

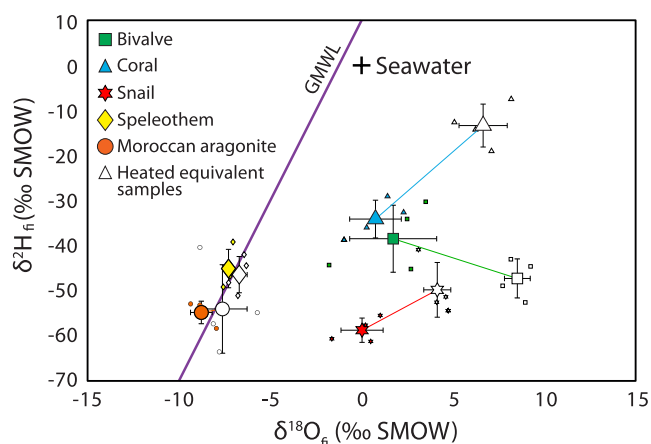


Figure 2. Cross-plot of $\delta^{18}\text{O}$ versus $\delta^2\text{H}$ values of fluid inclusions before and after heating. Large colored solid symbols represent the means of individual measurements (small symbols). White symbols mark the corresponding isotope compositions of heated subsample equivalents and their means are connected to the corresponding unheated values by lines. The statistical significance of changes in isotopic compositions before and after heating are reported in Table 1. The purple line represents the Global Meteoric Water Line (GMWL) and standard modern seawater is marked by a black cross.

confines of the CEF. Its value is calculated by the temperature equilibration of Bernasconi et al. (2018) at 175°C.

3. Results

3.1. Isotopic results

The isotopic results of the carbonate heating experiment are summarized in Table 1. The full data set is available in Data Set S1. The hydrogen and oxygen isotope composition of the fluid inclusions in inorganic carbonate samples correspond to the Global Meteoric Water Line (GMWL), whereas the biogenic aragonite samples are enriched in ^{18}O relative to the GMWL (Figure 2). The isotopic results of the fluid inclusion analysis of the speleothem sample are identical, within their uncertainties, to values reported by de Graaf et al. (2020). Clumped-isotope analyses of single-crystal “Moroccan” aragonite yield temperatures of 22°C and 20°C for unheated and heated samples, respectively, which are considered identical given the corresponding 95% confidence intervals of 16°C and 9°C, respectively. For the bivalve sample, temperatures of, respectively, 32°C and 70°C were obtained before and after heating. The 95% confidence intervals of these measurements correspond to uncertainties of 15°C and 19°C, respectively.

3.2. Statistical Significance of Isotopic Shifts

Significant thermal alteration occurred in hydrogen and oxygen isotopes in fluid inclusions, as well as in oxygen isotopes in calcite: the $\delta^2\text{H}_{\text{fi}}$ of the aragonitic coral shifted significantly from -34‰ to -13‰ (Table 1 and Figure 3). Significant ^{18}O enrichment of the $\delta^{18}\text{O}_{\text{fi}}$ composition was measured in the speleothem sample, but most pronounced isotopic shifts were recorded by the biogenic aragonite samples. Additionally, significant ^{18}O depletions were recorded for the speleothem calcite and the aragonite bivalve and coral, at a confidence interval of 95%. The $\delta^2\text{H}_{\text{fi}}$ values do not display a systemic shift after heating of speleothem, inorganic aragonite, bivalve and gastropod sample (Table 1). Clumped-isotope measurements record a significant shift ($p = 0.002$) in Δ_{47} and derived temperatures for the bivalve sample (Table 1 and Figure 4). In contrast, the Δ_{47} and associated temperatures of the inorganic “Moroccan” single-crystal aragonite sample remained unaffected by the heating treatment.

4. Discussion

4.1. Interpretation of Original Fluid Inclusion Composition

Although it was not the primary objective for this study, we are presenting the first analyses of fluid inclusion $\delta^2\text{H}$ and $\delta^{18}\text{O}$ values for many of the natural materials used in these experiments. Thus, some discussion will be given to possible signals in these observed values.

The hydrogen and oxygen compositions of the fluid inclusions of the inorganic samples match the GMWL (Figure 2), which supports a meteoric origin of these carbonate types and advocates the isotopic preservation of parental fluids. By contrast, the internal water in the biogenic samples distinctively deviates from the GMWL and the mean modern ocean water isotope composition. The terrestrial snail plots at the evaporative side of the GMWL, which is expected as the Δ_{47} growth temperatures in land snails are typically higher than ambient air temperatures (Guo et al., 2019). The fluid inclusion isotope composition of marine organisms is significantly different from seawater composition, especially the $\delta^2\text{H}$ composition, and appears to be controlled by the species-type, as was already observed by Lécuyer and O’Neil (1994). These deviations suggest that the composition of internal waters in biogenic samples was modified by species-specific metabolic processes.

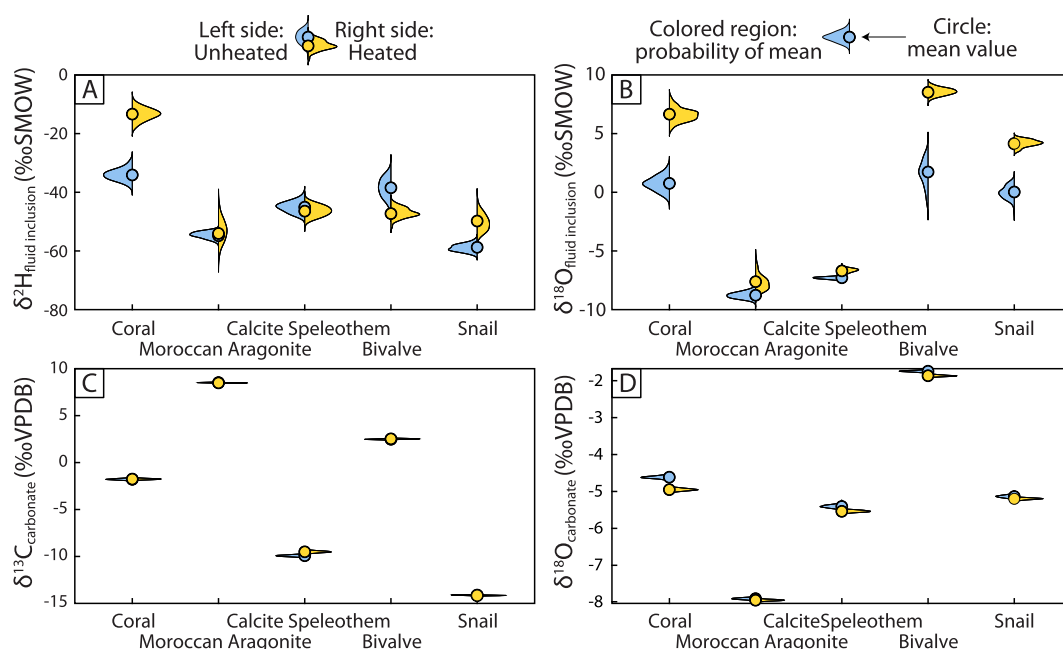


Figure 3. Violin plots showing the isotope distribution of heated and unheated sample data. Colored regions represent the probability distribution for mean values of unheated (left, blue) and heated (right, yellow). Filled circles represent the mean value for their respective data sets, represented by color. Upper panels (a and b) show the distribution of hydrogen and oxygen isotopic composition of the fluid inclusions in different biogenic and abiogenic carbonates, the lower panes (c and d) show the distribution of carbon and oxygen isotopic composition of the corresponding carbonate. Probability density functions calculated using bootstrap resampling of the measured data sets, and represent the confidence for the mean value for the entire sample's data set.

Analyses of coral aragonite via thermogravimetry and IR absorption indicate that much of the internal skeletal water is associated with an organic matrix (Cuif et al., 2004), much of which is internal to the minerals (intracrystalline organics in Figure 1b). Although the thermogravimetric experiments showed that the organically associated water is typically released at temperatures $\sim 300^{\circ}\text{C}$, it is possible that some of the water measured here was associated with these organics and thus represents a metabolically mediated origin. More research is needed to study the sources and significance of these different internal waters, and their differences between taxa.

4.2. Fluid Inclusion Isotopic Composition of Heated Materials

4.2.1. Leakage of Internal Water and/or Interference of Organic Matter

During the heating experiments, evaporated internal fluids may escape through microscopic fractures and openings as a result of increased fluid pressure. Even though the crushing efficiency (i.e., the particle size of the sample residue after crushing) varies between measurements, we find no direct evidence that the water released from heated samples (derived from the analytical intensity peaks; Data Set S1) was less than the water released from unheated samples. Also, isotopic evidence of partial evaporation, cooccurring significant excursions in heated samples toward positive $\delta^2\text{H}_{\text{fi}}$ and $\delta^{18}\text{O}_{\text{fi}}$ compositions with respect to unheated sample equivalents, were only detected in the coral sample (Table 1). The latter is in agreement with the heating experiment of Cuif et al. (2004), who indicated that as much as 0.5 wt.% water escapes from coral aragonite as it is heated to 200°C , a further <3 wt % of water is released with further heating above this temperature.

4.2.2. Interference of Organic Matter on Measured Fluid Inclusion Compositions

Decomposition of organic matter in biogenic carbonates is known to start at 100°C , potentially releasing its inter- and intracrystalline organic-bound fluids, H_2O and OH^- (Gaffey, 1988). The experiments presented by Cuif et al., (2004) indicate that, while water is released at lower temperatures, the water associated

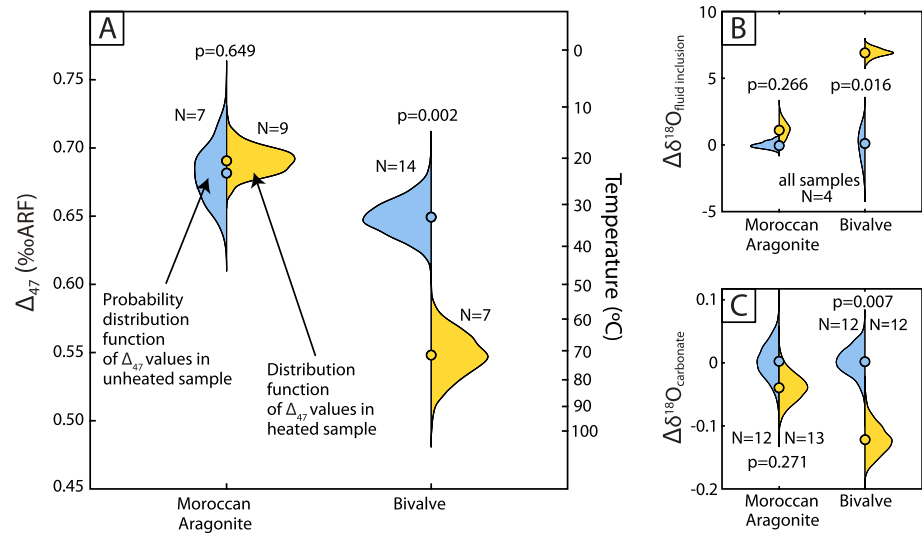


Figure 4. (a) Violin plot showing the difference in Δ_{47} values between unheated and heated samples for the inorganic “Moroccan” single-crystal aragonite sample and the bivalve aragonite sample. Colored regions represent the probability distribution for mean values of unheated (left, blue) and heated (right, yellow). Filled circles represent the mean value for their respective data sets, represented by color. The number of replicate analyses (N) is indicated for each sample set, along with the p value for the difference of means as determined by the t test. Corresponding temperature values are plotted on the secondary axis following the temperature calibration of Bernasconi et al. (2018). Panels (b and c) show the change in $\delta^{18}\text{O}$ values of fluid inclusions and carbonates between heated and unheated material, values in these panels have been normalized to the initial $\delta^{18}\text{O}$ value of the unheated material. Probability density functions calculated using bootstrap resampling of the measured data sets and represent the confidence for the mean value for the entire sample data set (Figure 5.)

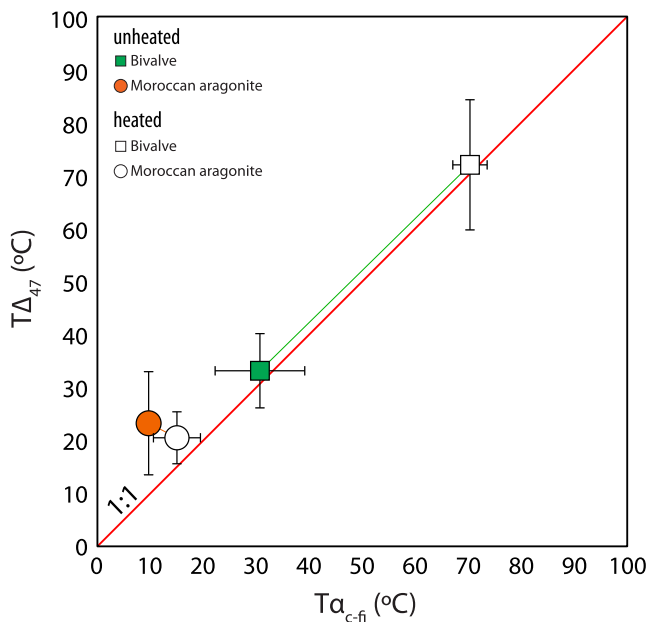


Figure 5. Resetting of the clumped-isotope paleothermometer versus the calcite-water paleothermometers. Shown are the results of the bivalve and inorganic aragonite sample, before and after the heating experiment. White symbols mark the isotope compositions of heated subsamples and are connected to the values of the unheated samples by lines. The red line indicates a 1:1 relation between paleothermometers.

with organic materials is generally released at $\sim 300^\circ\text{C}$, which is similar to the temperature required for the thermal transition from aragonite to calcite (Staudigel & Swart, 2016). Even if the organic-associated water is not being expelled, it may still be available for exchange reactions, however. Organic-associated water may potentially interfere with the fluid inclusion isotopic signal during sample analysis; crushing of the sample occurs in a heated chamber of 110°C and may thus already start to mobilize organically associated volatiles that affect the composition and $\alpha_{\text{c-fi}}$ values. Evidence for this process may be found in the cooccurring thermal decomposition of organic material, which also affects the $\delta^{13}\text{C}$ values of the carbonate measurements (Li et al., 2020). However, in the $\delta^{13}\text{C}$ analyses for this experiment, we find no evidence for the potential interference of organic matter, except in the speleothem sample, which may contain organic substances formed by bacteria or derived from soils (James et al., 1994; Ramseyer et al., 1997). However, even though the contribution of organic matter may go undetected, its effect on the isotopic composition may not be excluded and therefore, the initial hydrogen and oxygen compositions discussed in Section 4.1 should be interpreted carefully.

4.2.3. Oxygen Isotope Exchange Between Internal Water and Carbonate

During the experiment, oxygen responded to thermal alteration by becoming isotopically enriched in ^{18}O in the fluid phase and depleted in the carbonate phase. The positive shift in $\delta^{18}\text{O}_{\text{fi}}$ was recorded in all individual subsamples (Data Set S1; Figure 3b). Accordingly, a significant shift of the compositional mean of each sample type was recorded for each

sample type, except for the inorganic aragonite sample (Table 1). The shift toward higher $\delta^{18}\text{O}_{\text{fi}}$ values is likely the result of, at least partially, isotopic exchange between the carbonate and internal fluids; alteration of the $\delta^{18}\text{O}_{\text{fi}}$ composition in the biogenic aragonite samples may partially be caused by interference of organic tissue. However, the biogenic aragonite samples (the bivalve and coral) record associated compositional shifts toward more negative $\delta^{18}\text{O}_{\text{c}}$ values, strongly suggesting that isotope exchange between carbonate and fluid was the dominant process controlling the fractionation of oxygen isotopes.

4.2.4. Magnitude of Oxygen Isotope Shifts in Fluid Inclusions After Heating

The oxygen isotope exchange that we describe here was already determined experimentally for speleothem calcite by Uemura et al. (2019), who found that $\delta^{18}\text{O}_{\text{fi}}$ values increased by 0.7‰ after heating at 105 °C for over 80 h. In our study, we report a comparable 0.6‰ increase in $\delta^{18}\text{O}_{\text{fi}}$ for speleothem calcite sample after heating at 175 °C for 90 minutes. The isotopic increase of $\delta^{18}\text{O}_{\text{fi}}$ in the single-crystal inorganic aragonite sample remained within statistical uncertainty. Greater increases in the $\delta^{18}\text{O}_{\text{fi}}$ values were recorded in the biogenic aragonite samples between 4‰ and 6‰, indicating that biogenic samples experienced considerably more oxygen isotope exchange than inorganic calcite and aragonite.

Correspondingly, depletions in ^{18}O were measured in each carbonate subsample. Statistically significant changes in mean carbonate composition were recorded by the speleothem calcite, aragonite bivalve, coral and snail samples. The shift toward higher $\delta^{18}\text{O}_{\text{fi}}$ values and corresponding excursions toward negative $\delta^{18}\text{O}_{\text{c}}$ values in heated samples lead to higher equilibrium $\alpha_{\text{c-fi}}$ temperatures. The largest shifts of up to 40°C in $T_{\alpha_{\text{c-fi}}}$ were recorded in the biogenic aragonite samples (Table 1). Smaller temperature shifts of 4°C–5°C were recorded in inorganic materials.

4.2.5. Estimation of Internal Water Abundance

Equation 1 provides estimations of M_{f} based on the observed oxygen isotope exchange between calcite and fluid. The calculation of M_{f} was executed using a bootstrap-resampled Monte Carlo simulation, wherein measured values are resampled randomly for 100,000 iterations. This approach allows for the propagation of uncertainties from measured values to our final calculated values. It indicates that, assuming all internal fluids exchanged oxygen isotopes with the host carbonate, the coral, shell, and snail samples contained 3 ± 0.6 wt %, 0.9 ± 0.3 wt % and 0.8 ± 0.6 wt % of water, respectively ($\pm 95\%$ confidence of mean). Due to the small changes in fluid and carbonate $\delta^{18}\text{O}$ composition in the speleothem and single-crystal aragonite, it is challenging to accurately calculate the water percentages of the abiogenic materials; nevertheless, the same approach yields water contents of 11.4wt% and 2.7 wt%, respectively, with statistical uncertainties that exceed 100 wt% and thus are not considered to be significant. The excessively high uncertainties for the inorganic materials can be attributed to some permutations of the model having near-zero changes in fluid composition, which computes asymptotically large values for M_{f} , thus this approach is best used for samples with significant differences between initial and final compositions.

For the bivalve, where the CEF is constrained by clumped isotopes (4.3), the true M_{f} value can be adjusted to reflect the incomplete exchange between carbonates and fluids, giving a value of 1.0 ± 0.5 wt %, comparable to 0.9 ± 0.3 wt % without this correction. It must be noted that these estimates may be compromised if the oxygen isotopic signal was affected by interaction with organic tissue. Nevertheless, these values are roughly in agreement with previous estimates of the abundance of water in skeletal carbonates, which vary from several tenths of a percent up to 3 wt % (Gaffey, 1988).

4.3. Clumped-Isotope Resetting

In order to test the link between $\delta^{18}\text{O}$ exchange and Δ_{47} resetting, the bivalve and single-crystal aragonite samples were selected for clumped-isotope analyses. Results show that where the isotopic exchange is significant (in the bivalve sample), Δ_{47} decreases to reflect higher temperatures. In contrast, inorganic single-crystal aragonite, which did not record a significant response in $\delta^{18}\text{O}$ to heating, recorded no clumped-isotope alteration (Figure 4).

The experimental CEF (which is 0 if no carbonate is subjected to isotopic exchange and one if all carbonate is available for isotopic exchange with internal fluids) can be calculated based on the difference between the heated and unheated Δ_{47} values (Equation 3). For the single-crystal “Moroccan” aragonite, a

CEF is obtained of -0.003 ± 0.014 , whereas the aragonite bivalve shell yields a significantly larger CEF of 0.39 ± 0.07 (uncertainties represent $\pm 95\%$ confidence of mean). Evidence from experiments conducted at a range of temperatures by Staudigel and Swart (2016) shows an increase in the degree of exchange at higher temperatures, which may suggest that the CEF itself increases with temperature, and likely increases with time as well.

4.4. Difference in Exchange Potential Between Inorganic and Organic Carbonates?

The mechanism that facilitates the thermal reequilibration of $\delta^{18}\text{O}_f$ and $\delta^{18}\text{O}_c$ in carbonate minerals is also responsible for resetting the carbonate Δ_{47} -temperatures. Yet, the process that causes these exchange reactions to occur is not easily identified, as the exchange of oxygen isotopes and resetting of Δ_{47} values occurs without a detectable transition of aragonite to calcite (Figure S1; Data Set S1), a result which has been noted in previous studies (Grossman et al., 1986; Moon et al., 2020; Müller, Staudigel, et al., 2017; Ritter et al., 2017; Staudigel & Swart, 2016). To our knowledge, there are two ways in which to reset clumped-isotope temperatures; via recrystallization and solid-state reordering. It was recently advocated that this form of reordering in biogenic aragonite may act at lower temperatures than initially observed, possibly driven by the freeze-thaw cycle during early burial (Wang et al., 2020); a process which Wang et al. (2020) argued was accompanied with minor changes from aragonite to calcite. If these observations are correct, then there may be additional internal reactions at lower temperatures, which may liberate water for exchange with carbonate or facilitate similar exchange reactions.

It is conceivable that microscale dissolution-precipitation reactions occur at an internal carbonate-fluid interface, but below current detection limits. Thus, the geometry of pores, and surface area in particular, may be an important predictor for the relative fraction of available carbonate for exchange with a pore (CEF-value). High-resolution investigation of fresh calcite cleavage surfaces revealed that the calcite surfaces are highly dynamic and recrystallization reactions occur continuously at the surface, even when we consider a surface dry (Chiarello et al., 1993; Stipp et al., 1996). This process may have very minor effects when the carbonate crystal is considered “closed” and the contact surface between fluid inclusions and the host mineral is small. Biogenic aragonites contain a network of internal hydrated organic matter, which can destabilize at elevated temperatures (Cuif et al., 2004; Dauphin et al., 2006); anisotropic lattice distortions of the mineral phase, believed to be caused by these proteins, tend to anneal at temperatures between 125 and 200 °C (Pokroy et al., 2006). It is unclear at this time if this crystalline annealing is associated with oxygen exchange between the carbonate phase. It is, however, possible that the hydrated organic matrix in biogenic carbonates (Figure 1b) in some way accounts for an increased pore-surface contact area relative to inorganic carbonates, effectively creating an increased potential for isotopic exchange. It has further been suggested that, after the loss of interlamellar (intercrystalline in Figure 1b) organic tissue during oxidation and fossilization, internal water remains predominantly present within aragonite crystals of the nacreous layers of molluscs (Hudson, 1967).

4.5. Implications

The susceptibility of biogenic aragonite to alteration at elevated temperatures has been demonstrated to be important in settings such as laboratory sampling (Staudigel & Swart, 2016) as well as during the roasting of archeological midden components (Müller, Staudigel, et al., 2017; Staudigel et al., 2019). Here, we present an experiment, which provides a substantial improvement to our mechanistic understanding of what drives these alteration processes. Even though the results of this study were only significant for biogenic aragonite, we hypothesize that the same process can also apply to biogenic calcite, as well as inorganic calcite and aragonite, albeit possibly at a lower rate. Although experimental thermal alteration resulted in changes in isotopic composition within the analytical uncertainty for inorganic aragonite, we suggest that the same process could significantly affect inorganic calcite and aragonite on geological timescales, having consequences for researchers that study calcite veins. Our results show that analyses of trapped fluid $\delta^{18}\text{O}$ values, in conjunction with carbonate clumped isotopes, can be used to better understand these internal alteration processes; this has the potential to be applied to identify samples that have undergone such exchange processes during heating in future studies.

Because clumped-isotope resetting in biogenic aragonites occurs at much lower temperatures than those required for solid-state reordering on the same timescales (Henkes et al., 2014; Passey & Henkes, 2012) and the aragonite-calcite phase transition (Chen et al., 2019; Staudigel & Swart, 2016), we hypothesize that this process operates prior to and alongside solid-state reordering. During a simple burial heating scenario (i.e., temperatures increasing over time), these fluid-carbonate exchange reactions would be expected to occur prior to solid-state reordering. This implies as well that Δ_{47} -resetting that was previously attributed to solid-state reordering, may have partly been caused by internal isotope exchange reactions at the carbonate-fluid interface. For instance, the observed initial exponential reaction of Δ_{47} to heating in solid-state reordering experiments that was first ascribed to annealing of crystalline defects (Passey & Henkes, 2012) and later to solid-state isotope exchange between neighboring carbonate ions (Stolper & Eiler, 2015), may be influenced by the mechanism described here in carbonates with internal water available for exchange.

5. Conclusion

Our experiments show that the oxygen isotope composition of biogenic aragonites can be affected by heating below the threshold for the aragonite-calcite transition, a commonly used indicator for diagenetic alteration. By means of a dry heating experiment (175°C for 90 minutes), we show that this alteration, which typically results in a shift toward negative $\delta^{18}\text{O}$ values of the host carbonate, is caused by the interaction between host carbonate and internal fluids. The response to this heating differs between carbonate materials; the isotopic composition of various types of biogenic aragonite samples show significant changes in the isotopic composition of both fluid inclusions and host carbonate, while inorganic aragonite and calcite samples do not. The occurrence of this isotopic exchange is linked also to the resetting of Δ_{47} values, suggesting that the reequilibration of oxygen isotopes and resetting of Δ_{47} -composition is caused by the same process. We suggest that the magnitude of isotope exchange and Δ_{47} -resetting depends on the amount of CaCO_3 available for isotopic exchange, a fraction that is defined as the CEF, and that this fraction varies among different materials. Studied samples show that inorganic aragonite and speleothem calcite were virtually unaffected by the experimental treatment, while the same treatment resulted in resetting of Δ_{47} values in 39% of the aragonitic bivalve sample. Possibly, microscale dissolution-precipitation reactions at the carbonate-fluid interface are the cause of the coupled alteration of clumped and oxygen isotopes, even in the absence of visible signs of alteration. The shape and distribution of internal fluid inclusions and organic-bound fluids may play an important role in determining the carbonate-fluid reaction surface, creating the differences in diagenetic response between organic and inorganic carbonates. The results presented here shed light on an otherwise cryptic diagenetic process, which affects the isotopic composition, but does not measurably affect the initial mineralogy of biogenic aragonites, highlighting the importance of coupling clumped-isotope analyses with data from other measured proxies. These results raise the question of whether observations attributed to specific clumped-isotope behaviors, such as solid-state reordering or the observed initial exponential reaction of Δ_{47} to experimental heating, may be influenced by the mechanism described here instead. The effects of this process should be considered by researchers studying clumped-isotope composition of fossil aragonite archives, but our results may have broader-reaching implications for those working on calcite fossils and inorganic carbonates.

Acknowledgments

The idea for this study was fueled by the research conducted during PTS's PhD thesis, therefore the authors acknowledge the intellectual contribution of Peter Swart, his PhD supervisor. The authors are deeply grateful for the efforts and support of John Reijmer, who supervises the first author's PhD. The authors are thankful to Suzan Verdegaaal for the technical support and analyses of stable isotope data at the Earth Sciences Stable Isotope Laboratory at Vrije Universiteit Amsterdam (The Netherlands). Furthermore, the authors very much appreciate XRD analyses that were performed by João Trabucho Alexandre (UU) and Anthony Oldroyd (Cardiff School of Earth and Environmental Sciences). M. Ziegler acknowledges funding through the NWO VIDI project 016.161.365, which is financed by the Netherlands Organization for Scientific Research (NWO). This study is part of the first author's PhD thesis.

Data Availability Statement

The supporting information (Data Sets S1 and S2) are available as Excel 2007 spreadsheets (ds01.xlsx and ds02.xlsx) with the online version of this manuscript and at Harvard Dataverse (<https://doi.org/10.7910/DVN/YMCH51>).

References

- Adabi, M. H. (2004). A re-evaluation of aragonite versus calcite seas. *Carbonates and Evaporites*, 19(2), 133–141. <https://doi.org/10.1007/BF03178476>
- Balthasar, U., & Cusack, M. (2015). Aragonite-calcite seas-Quantifying the gray area. *Geology*, 43(2), 99–102. <https://doi.org/10.1130/G36293.1>
- Bernasconi, S. M., Müller, I. A., Bergmann, K. D., Breitenbach, S. F. M., Fernandez, A., Hodell, D. A., et al. (2018). Reducing uncertainties in carbonate clumped isotope analysis through consistent carbonate-based standardization. *Geochemistry, Geophysics, Geosystems*, 19, 2895–2914. <https://doi.org/10.1029/2017GC007385>

- Bischoff, J. L., & Fyfe, W. S. (1968). Catalysis, inhibition, and the calcite-aragonite problem. [Part] 1: The aragonite-calcite transformation. *American Journal of Science*, 266(2), 65–79. <https://doi.org/10.2475/ajs.266.2.65>
- Brand, W. A., Assonov, S. S., & Coplen, T. B. (2010). Correction for the ^{17}O interference in $\delta^{13}\text{C}$ measurements when analyzing CO_2 with stable isotope mass spectrometry (IUPAC Technical Report). *Pure and Applied Chemistry*, 82(8), 1719–1733. <https://doi.org/10.1351/PAC-REP-09-01-05>
- Carlson, W. D. (1980). The calcite-aragonite equilibrium: Effects of Sr substitution and anion orientational disorder | American Mineralogist | GeoScienceWorld. *American Mineralogist*, 65(11–12), 1252–1262.
- Casella, L. A., Griesshaber, E., Yin, X., Ziegler, A., Mavromatis, V., Müller, D., et al. (2017). Experimental diagenesis: Insights into aragonite to calcite transformation of Arctic islandica shells by hydrothermal treatment. *Biogeosciences*, 14, 1461–1492. <https://doi.org/10.5194/bg-14-1461-2017>
- Chen, S., Ryb, U., Piasecki, A. M., Lloyd, M. K., Baker, M. B., & Eiler, J. M. (2019). Mechanism of solid-state clumped isotope reordering in carbonate minerals from aragonite heating experiments. *Geochimica et Cosmochimica Acta*, 258, 156–173. <https://doi.org/10.1016/j.gca.2019.05.018>
- Chiarello, R. P., Wogelius, R. A., & Sturchio, N. C. (1993). In-situ synchrotron X-ray reflectivity measurements at the calcite-water interface. *Geochimica et Cosmochimica Acta*, 57(16), 4103–4110. [https://doi.org/10.1016/0016-7037\(93\)90356-2](https://doi.org/10.1016/0016-7037(93)90356-2)
- Coplen, T. B. (2007). Calibration of the calcite-water oxygen-isotope geothermometer at Devils Hole, Nevada, a natural laboratory. *Geochimica et Cosmochimica Acta*, 71(16), 3948–3957. <https://doi.org/10.1016/J.GCA.2007.05.028>
- Cuif, J.-P., Dauphin, Y., Berthet, P., & Jegoudez, J. (2004). Associated water and organic compounds in coral skeletons: Quantitative thermogravimetry coupled to infrared absorption spectrometry. *Geochemistry, Geophysics, Geosystems*, 5, Q11011. <https://doi.org/10.1029/2004GC000783>
- Daëron, M., Blamart, D., Peral, M., & Affek, H. P. (2016). Absolute isotopic abundance ratios and the accuracy of $\Delta 47$ measurements. *Chemical Geology*, 442(441), 83–96. <https://doi.org/10.1016/j.chemgeo.2016.08.014>
- Daëron, M., Drysdale, R. N., Peral, M., Huyghe, D., Blamart, D., Coplen, T. B., et al. (2019). Most Earth-surface calcites precipitate out of isotopic equilibrium. *Nature Communications*, 10, 429. <https://doi.org/10.1038/s41467-019-08336-5>
- Dauphin, Y., Cuif, J.-P., & Massard, P. (2006). Persistent organic components in heated coral aragonitic skeletons: Implications for palaeoenvironmental reconstructions. *Chemical Geology*, 231, 26–37. <https://doi.org/10.1016/j.chemgeo.2005.12.010>
- de Graaf, S., Vonhof, H. B., Weissbach, T., Wassenburg, J. A., Levy, E. J., Kluge, T., & Haug, G. H. (2020). A comparison of isotope ratio mass spectrometry and cavity ring-down spectroscopy techniques for isotope analysis of fluid inclusion water. *Rapid Communications in Mass Spectrometry*, 34(16), e8837. <https://doi.org/10.1002/rcm.8837>
- Folk, R. L. (1965). Some aspects of recrystallization in ancient limestones. In *Dolomitization and limestone diagenesis* (pp. 14–48). Tulsa, OK: SEPM (Society for Sedimentary Geology). <https://doi.org/10.2110/pec.65.07.0014>
- Gaffey, S. J. (1988). Water in skeletal carbonates. *Journal of Sedimentary Petrology*, 58(3), 397–414. <https://doi.org/10.1306/212f8da5-2b24-11d7-8648000102c1865d>
- Gat, J. R., & Gonfiantini, R. (1981). *Stable isotope hydrology. Deuterium and oxygen-18 in the water cycle* (Tech. Rep. Ser. 210). Vienna: International atomic energy agency.
- Grossman, E. L., Betzer, P. R., Dudley, W. C., & Dunbar, R. B. (1986). Stable isotopic variation in pteropods and Atlantids from North Pacific sediment traps. *Marine Micropaleontology*, 10(1–3), 9–22. [https://doi.org/10.1016/0377-8398\(86\)90022-8](https://doi.org/10.1016/0377-8398(86)90022-8)
- Guo, Y., Deng, W., Wei, G., Lo, L., & Wang, N. (2019). Clumped isotopic signatures in land-snail shells revisited: Possible palaeoenvironmental implications. *Chemical Geology*, 519, 83–94. <https://doi.org/10.1016/j.chemgeo.2019.04.030>
- Hacker, B. R. (2005). The calcite → aragonite transformation in low-Mg marble: Equilibrium relations, transformation mechanisms, and rates. *Journal of Geophysical Research*, 110, B03205. <https://doi.org/10.1029/2004JB003302>
- Henkes, G. A., Passey, B. H., Grossman, E. L., Shenton, B. J., Pérez-Huerta, A., & Yancey, N. (2014). Temperature limits for preservation of primary calcite clumped isotope paleotemperatures. *Geochimica et Cosmochimica Acta*, 139, 362–382. <https://doi.org/10.1016/j.gca.2014.04.040>
- Hudson, J. D. (1967). The elemental composition of the organic fraction, and the water content, of some recent and fossil mollusc shells. *Geochimica et Cosmochimica Acta*, 31, 2361–2378. [https://doi.org/10.1016/0016-7037\(67\)90008-7](https://doi.org/10.1016/0016-7037(67)90008-7)
- James, J. M., Patsalides, E., & Cox, G. (1994). Amino acid composition of stromatolitic stalagmites. *Geomicrobiology Journal*, 12(3), 183–194. <https://doi.org/10.1080/01490459409377985>
- Kim, S.-T., & O’Neil, J. R. (1997). Equilibrium and nonequilibrium oxygen isotope effects in synthetic carbonates. *Geochimica et Cosmochimica Acta*, 61(16), 3461–3475. [https://doi.org/10.1016/S0016-7037\(97\)00169-5](https://doi.org/10.1016/S0016-7037(97)00169-5)
- Kocken, I. J., Müller, I. A., & Ziegler, M. (2019). Optimizing the use of carbonate standards to minimize uncertainties in clumped isotope data. *Geochemistry Geophysics Geosystems*, 20, 5565–5577. <https://doi.org/10.1029/2019GC008545>
- Lécuyer, C., & O’Neil, J. R. (1994). Stable isotope compositions of fluid inclusions in biogenic carbonates. *Geochimica et Cosmochimica Acta*, 58(1), 353–363. [https://doi.org/10.1016/0016-7037\(94\)90469-3](https://doi.org/10.1016/0016-7037(94)90469-3)
- Li, C., Shen, H., Sheng, X., Wei, H., & Chen, J. (2020). Kinetics and fractionation of carbon and oxygen isotopes during the solid-phase transformation of biogenic aragonite to calcite: The effect of organic matter. *Palaeogeography, Palaeoclimatology, Palaeoecology*, 556, 109876. <https://doi.org/10.1016/j.palaeo.2020.109876>
- Meckler, A. N., Ziegler, M., Millán, M. I., Breitenbach, S. F. M., & Bernasconi, S. M. (2014). Long-term performance of the Kiel carbonate device with a new correction scheme for clumped isotope measurements. *Rapid Communications in Mass Spectrometry*, 28(15), 1705–1715. <https://doi.org/10.1002/rcm.6949>
- Milano, S., Lindauer, S., Prendergast, A. L., Hill, E. A., Hunt, C. O., Barker, G., & Schöne, B. R. (2018). Mollusk carbonate thermal behavior and its implications in understanding prehistoric fire events in shell middens. *Journal of Archaeological Science: Reports*, 20, 443–457. <https://doi.org/10.1016/j.jasrep.2018.05.027>
- Milano, S., Prendergast, A. L., & Schöne, B. R. (2016). Effects of cooking on mollusk shell structure and chemistry: Implications for archeology and paleoenvironmental reconstruction. *Journal of Archaeological Science: Reports*, 7, 14–26. <https://doi.org/10.1016/j.jasrep.2016.03.045>
- Moon, L. R., Judd, E. J., Thomas, J., & Ivany, L. C. (2020). Out of the oven and into the fire: Unexpected preservation of the seasonal d^{18}O cycle following heating experiments on shell carbonate. *Palaeogeography, Palaeoclimatology, Palaeoecology*, 254, 117433. <https://doi.org/10.1016/j.carbpol.2020.117433>
- Müller, I. A., Fernandez, A., Radke, J., van Dijk, J., Bowen, D., Schwieters, J., & Bernasconi, S. M. (2017). Carbonate clumped isotope analyses with the long-integration dual-inlet (LIDI) workflow: Scratching at the lower sample weight boundaries. *Rapid Communications in Mass Spectrometry*, 31(12), 1057–1066. <https://doi.org/10.1002/rcm.7878>

- Müller, P., Staudigel, P. T., Murray, S. T., Vernet, R., Barusseau, J.-P., Westphal, H., & Swart, P. K. (2017). Prehistoric cooking versus accurate paleotemperature records in shell midden constituents. *Scientific Reports*, 7(1), 1–11. <https://doi.org/10.1038/s41598-017-03715-8>
- Nooitgedacht, C., van der Lubbe, H., De Graaf, S., Ziegler, M., Staudigel, P., & Reijmer, J. J. G. (2021). Restricted internal oxygen isotope exchange in calcite veins: Constraints from fluid inclusion and clumped isotope-derived temperatures. *Geochimica et Cosmochimica Acta*, 297, 24–39. <https://doi.org/10.1016/j.gca.2020.12.008>
- Passey, B. H., & Henkes, G. A. (2012). Carbonate clumped isotope bond reordering and geospeedometry. *Earth and Planetary Science Letters*, 351–352, 223–236. <https://doi.org/10.1016/j.epsl.2012.07.021>
- Pederson, C., Mavromatis, V., Dietzel, M., Rollion-Bard, C., Nehrke, G., Jöns, N., et al. (2019). Diagenesis of mollusc aragonite and the role of fluid reservoirs. *Earth and Planetary Science Letters*, 514, 130–142. <https://doi.org/10.1016/j.epsl.2019.02.038>
- Pederson, C. L., Mavromatis, V., Dietzel, M., Rollion-Bard, C., Breitenbach, S. F. M., Yu, D., et al. (2020). Variation in the diagenetic response of aragonite archives to hydrothermal alteration. *Sedimentary Geology*, 406, 105716. <https://doi.org/10.1016/j.sedgeo.2020.105716>
- Pederson, C. L., Weiss, L., Mavromatis, V., Rollion-Bard, C., Dietzel, M., Neuser, R., & Immenhauser, A. (2019). Significance of fluid chemistry throughout diagenesis of aragonitic Porites corals—An experimental approach. *The Depositional Record*, 5(3), 592–612. <https://doi.org/10.1002/dep2.82>
- Pokroy, B., Fitch, A. N., Lee, P. L., Quintana, J. P., Caspi, E. A. N., & Zolotoyabko, E. (2006). Anisotropic lattice distortions in the mollusk-made aragonite: A widespread phenomenon. *Journal of Structural Biology*, 153(2), 145–150. <https://doi.org/10.1016/j.jsb.2005.10.009>
- Ramseyer, K., Miano, T. M., D'orazio, V., Wildberger, A., Wagner, T., & Geister, J. (1997). Nature and origin of organic matter in carbonates from speleothems, marine cements and coral skeletons. *Organic Geochemistry*, 26(5–6), 361–378. [https://doi.org/10.1016/S0146-6380\(97\)00008-9](https://doi.org/10.1016/S0146-6380(97)00008-9)
- Ritter, A.-C., Mavromatis, V., Dietzel, M., Kwicien, O., Wiethoff, F., Griesshaber, E., et al. (2017). Exploring the impact of diagenesis on (isotope) geochemical and microstructural alteration features in biogenic aragonite. *Sedimentology*, 64, 1354–1380. <https://doi.org/10.1111/sed.12356>
- Sandberg, P. A. (1983). An oscillating trend in Phanerozoic non-skeletal carbonate mineralogy. *Nature*, 305(5929), 19–22. <https://doi.org/10.1038/305019a0>
- Stahl, W., & Jordan, R. (1969). General considerations on isotopic paleotemperature determinations and analyses on Jurassic ammonites. *Earth and Planetary Science Letters*, 6(3), 173–178. [https://doi.org/10.1016/0012-821X\(69\)90086-7](https://doi.org/10.1016/0012-821X(69)90086-7)
- Staudigel, P. T., & Swart, P. K. (2016). Isotopic behavior during the aragonite-calcite transition: Implications for sample preparation and proxy interpretation. *Chemical Geology*, 442, 130–138. <https://doi.org/10.1016/j.chemgeo.2016.09.013>
- Staudigel, P. T., & Swart, P. K. (2018). A kinetic difference between ¹²C- and ¹³C-bound oxygen exchange rates results in decoupled δ¹⁸O and Δ47 values of equilibrating DIC solutions. *Geochemistry Geophysics Geosystems*, 19, 2371–2383. <https://doi.org/10.1029/2018GC007500>
- Staudigel, P. T., Swart, P. K., Pourmand, A., Laguer-Diaz, C. A., & Pestle, W. J. (2019). Boiled or roasted? Bivalve cooking methods of early Puerto Ricans elucidated using clumped isotopes. *Science Advances*, 5(11), 5447–5474. <https://doi.org/10.1126/sciadv.aaw5447>
- Stipp, S. L. S., Gutmannsbauer, W., & Lehmann, T. (1996). The dynamic nature of calcite surfaces in air. *American Mineralogist*, 81(1–2), 1–8. <https://doi.org/10.2138/am-1996-1-201>
- Stolper, D. A., & Eiler, J. M. (2015). The kinetics of solid-state isotope-exchange reactions for clumped isotopes: A study of inorganic calcites and apatites from natural and experimental samples. *American Journal of Science*, 315(5), 363–411. <https://doi.org/10.2475/05.2015.01>
- Tremaine, D. M., Froelich, P. N., & Wang, Y. (2011). Speleothem calcite farmed in situ: Modern calibration of δ¹⁸O and δ¹³C paleoclimate proxies in a continuously-monitored natural cave system. *Geochimica et Cosmochimica Acta*, 75(17), 4929–4950. <https://doi.org/10.1016/j.gca.2011.06.005>
- Uemura, R., Kina, Y., & Omine, K. (2019). Experimental evaluation of oxygen isotopic exchange between inclusion water and host calcite in speleothems. *Climate of the Past Discussions*, 3, 1–18. <https://doi.org/10.5194/cp-2019-79>
- Vonhof, H. B., Van Breukelen, M. R., Postma, O., Rowe, P. J., Atkinson, T. C., & Kroon, D. (2006). A continuous-flow crushing device for on-line δ²H analysis of fluid inclusion water in speleothems. *Rapid Communications in Mass Spectrometry*, 20(17), 2553–2558. <https://doi.org/10.1002/rcm.2618>
- Wang, Y., Passey, B., Roy, R., Deng, T., Jiang, S., Hannold, C., et al. (2020). Clumped isotope thermometry of modern and fossil snail shells from the Himalayan-Tibetan Plateau: Implications for paleoclimate and paleoelevation reconstructions. *Geological Society of America Bulletin*. <https://doi.org/10.1130/b35784.1>
- Yan, H., Sun, H., & Liu, Z. (2012). Equilibrium vs. kinetic fractionation of oxygen isotopes in two low-temperature travertine-depositing systems with differing hydrodynamic conditions at Baishuitai, Yunnan, SW China. *Geochimica et Cosmochimica Acta*, 95, 63–78. <https://doi.org/10.1016/j.gca.2012.07.024>
- Zhang, S., Zhou, R., & DePaolo, D. J. (2020). The seawater Sr/Ca ratio in the past 50 Myr from bulk carbonate sediments corrected for diagenesis. *Earth and Planetary Science Letters*, 530, 115949. <https://doi.org/10.1016/j.epsl.2019.115949>